CrossMark

# A Graphene-Based Terahertz Hot Electron Bolometer with Johnson Noise Readout

W. Miao[1,2] · H. Gao[1,2] · Z. Wang[1,2] · W. Zhang[1,2] ·
Y. Ren[1,2] · K. M. Zhou[1,2] · S. C. Shi[1,2] · C. Yu[3] ·
Z. Z. He[3] · Q. B. Liu[3] · Z. H. Feng[3]

**Abstract** In this paper, we present the development of a graphene-based hot electron bolometer with Johnson noise readout. The bolometer is a graphene microbridge connected to a log spiral antenna by Au contact pads. The Fourier transform spectrometer measurement shows the bolometer has high coupling efficiency in the frequency range from 0.3 to 1.6 THz. Using 300/77 K blackbody loads, we measure an optical noise equivalent power of $5.6 \times 10^{-12}$ W/Hz$^{0.5}$ at 3.0 K. To understand the thermal transport inside the graphene microbridge, we measure the bolometers with different microbridge lengths at different bath temperatures. We find that the thermal conductance due to electron diffusion is significant in the bolometers.

## 1 Introduction

It is well known that graphene has extremely weak electron–phonon coupling [1] and strong Drude absorption of terahertz radiation [2]. These remarkable properties make graphene very attractive for hot electron bolometers (HEBs) at terahertz frequencies. However, the resistance of graphene has a weak temperature dependence that limits the ultimate sensitivity of graphene with resistive readout. To achieve a strong tem-

✉ S. C. Shi
scshi@mail.pmo.ac.cn

1    Purple Mountain Observatory, CAS, Nanjing 210008, China

2    Key Lab of Radio Astronomy, CAS, Nanjing 210008, China

3    Hebei Semiconductor Research Institute, Shijiazhuang 050051, China

perature dependence, several attempts have been made by using nano-patterned dots of graphene [3], by introducing defects to induce strong localization [4] or by using a superconducting tunnel junction [5]. All these schemes have successfully realized extremely high electrical responsivity for graphene-based HEBs at low temperatures. A different technique to probe the thermal transport and electron temperature of graphene is noise thermometry [6, 7]. Based on this technique, the potential of graphene-based HEBs with high sensitivity has been demonstrated in Ref. 6. In this work, we report on the development of a graphene-based THz hot electron bolometer with noise thermometry. Its noise equivalent power (NEP) and the dependence on microbridge size and bath temperature are studied.

## 2 Graphene-Based HEB and Experimental Setup

Figure 1a shows the image of the investigated graphene-based hot electron bolometer. It consists of a 2-$\mu$m-long and 10-$\mu$m-wide graphene microbridge connected to a log spiral antenna by Au contact pads. The antenna has an outer diameter of 400 $\mu$m and an inner diameter of 13 $\mu$m and is expected to cover 0.1–1.4 THz [8]. The fabrication process of the HEB device starts from the growth of epitaxial graphene on a 4H–SiC substrate. During the process, silicon vapor and argon inert gas are introduced as background atmosphere to ensure good crystal quality. Then the HEB device is fabricated by optical lithography and standard lift off process. The fabricated HEB device has a dc resistance of 75 $\Omega$ at 300 K and 60 $\Omega$ at 3.0 K.

We investigated the characteristics of the graphene-based HEB with a 3 K pulse tube cooler and a 0.3 K Gifford–McMahon/sorption cooler. The pulse tube cooler has a 1.0-mm-thick high-density polyethylene window and a Zitex G104 infrared filter. The Gifford–McMahon/sorption cooler has no optical window and is only used to study the electrical characteristics of the HEB. The HEB device is glued to an elliptical Si lens and is mounted to a copper block anchored on the cold plate of the cooler. The HEB is read out by measuring its noise power in the frequency range from 2 to 4 GHz. The noise power is amplified by a cryogenic low noise amplifier and then by two room-temperature amplifiers. Last the noise power is recorded by a square law detector of a sensitivity of 1 mV/$\mu$W.

## 3 Temperature Dependence of Noise Power

The HEB was first measured in the 0.3 K Gifford–McMahon/sorption cooler. Figure 2 (left) shows the measured noise power variation as a function of dc input power at different bath temperatures. Here the dominant noise sources are the Johnson noise of the bolometer and the readout noise. The noise power can be written as $P_{out} = k_B(T_e + T_{readout})G_{LNA}B$, where $T_e$ and $T_{readout}$ are the electron temperature of graphene and the equivalent noise temperature of readout system, respectively, $G_{LNA}$ is the gain of the amplifiers, and $B$ is the noise bandwidth. According to Fig. 2 (left), it can be seen that the lower the bath temperature is, the larger the slope of noise power variation appears at the lower dc power regime. At 0.3 and 3.0 K, the initial slopes of noise power variation $dP_{out}/P_{in}|P_{in} \rightarrow 0$ are around 0.63 and 0.09 $\mu$W/nW, respectively. Figure 2
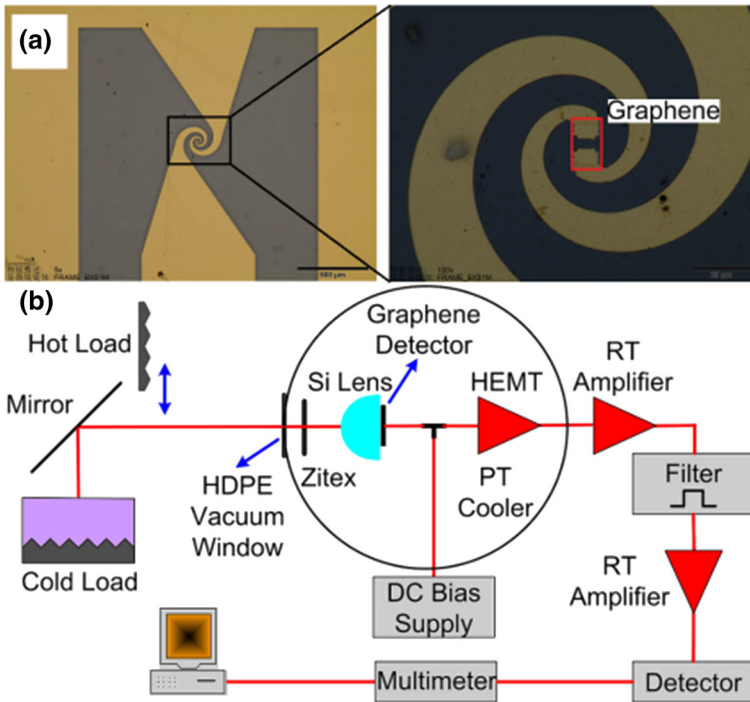
**Fig. 1 a** Image of the graphene-based hot electron bolometer. **b** Schematic diagram of the experimental setup with a 3 K pulse tube cooler, where 300/77 K blackbody loads are used for optical NEP measurement (Color figure online)

(right) shows the measured noise power of the HEB as a function of bath temperature. A linear fitting to the measured data yields a slope of noise power with respect to temperature of $dP_{out}/dT_e = 0.64 \, \mu$W/K. From this temperature dependence, we can estimate the thermal resistance of the HEB $dT_e/P_{in}|P_{in} \rightarrow 0 = 1$ K/nW at 0.3 K. It is lower than the result in Ref. 4 where the electron diffusion cooling is suppressed by using a Boron Nitride tunneling barrier. In addition, one can obtain the readout noise temperature $T_{readout}$ from the cross-point of the linear fitting and the temperature axis. In this case, the readout noise temperature is estimated to be $12.8 \pm 0.1$ K if a good impedance match between the HEB and the cryogenic low noise amplifier is assumed.

## 4 Frequency Response and Noise Equivalent Power

We then mounted the graphene-based HEB in the 3 K pulse tube cooler and measured its frequency response with a Fourier transform spectrometer (FTS). The FTS was operated in a step-and-integrate mode, and the noise power of the HEB was recorded by a lock-in amplifier that is synchronized with a chopper used for the modulation of the radiation signal. Figure 3 (left) shows the measured frequency response of the HEB, and the inset is the measured interferogram. It can be seen that the graphene-based HEB has high coupling efficiency in the frequency range of 0.3–1.6 THz. Here the measured frequency response is mainly determined by the coupling between the
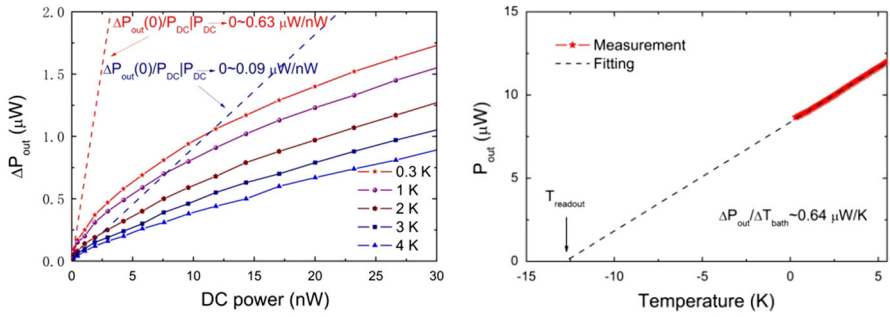
**Fig. 2** (Left) measured noise power variation as a function of dc power at different bath temperatures. (Right) measured noise power of the HEB as a function of bath temperature (Color figure online)
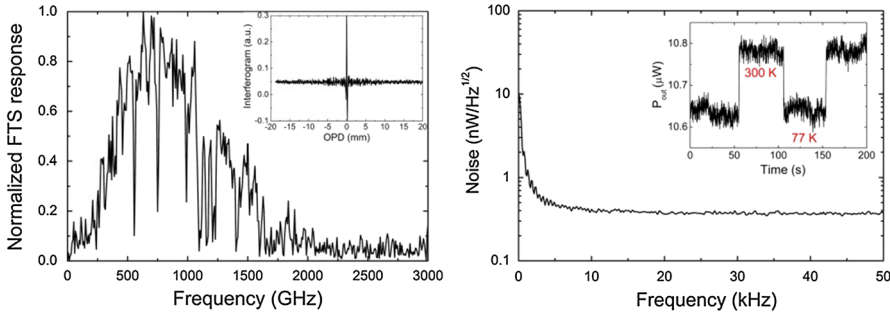


**Fig. 3** (Left) measured frequency response of the graphene-based HEB. The inset is the measured interferogram. (Right) measured noise spectrum of the noise power of the HEB at 3.0 K. The inset is the noise power (with hot and cold loads altered) versus time (Color figure online)

log spiral antenna and the graphene microbridge and by the FTS system itself. Figure 3 (right) shows the measured noise spectrum of the noise power of the HEB (at zero bias) at 3.0 K. At frequencies above 10 kHz, the noise spectrum is nearly flat and is about 0.36 nW/Hz$^{1/2}$. At low frequencies, the 1/$f$ noise might be due to the temperature fluctuation and mechanical vibration of the pulse tube cooler. The inset of Fig. 3 (right) shows the measured noise power of the HEB for altered 300 and 77 K blackbody loads. The change in the noise power for altered loads is found to be ∼0.16 μW. In this case, the difference of incident power on the HEB is estimated as $\eta \int (\varepsilon(f, T_{\text{hot}}) - \varepsilon(f, T_{\text{cold}}))\mathrm{d}f$, where $\varepsilon(f, T) = hf/(e^{hf/kT} - 1)$ is single mode blackbody power spectrum density, and $\eta$ is the coupling efficiency that includes the contribution from vacuum window (0.93), IR filter (0.95) and Si lens reflection (0.71). In the frequency range of 0.3–1.6 THz, the incident power difference is estimated to be ∼2.48 nW. In combination with the measured noise power change and noise spectrum density, the optical NEP of the graphene-based HEB is found to be $5.6 \times 10^{-12}$ W/Hz$^{0.5}$ at 3.0 K.

According to the Dicke formula, the NEP of a graphene-based HEB based on Johnson noise readout can be described as [9]

$$\text{NEP}_{\text{JNT}} = \frac{(T_{\text{e}} + T_{\text{readout}})\left(G_{\text{e-ph}} + G_{\text{diff}} + G_{\gamma}\right)}{\sqrt{2B}}, \tag{1}$$
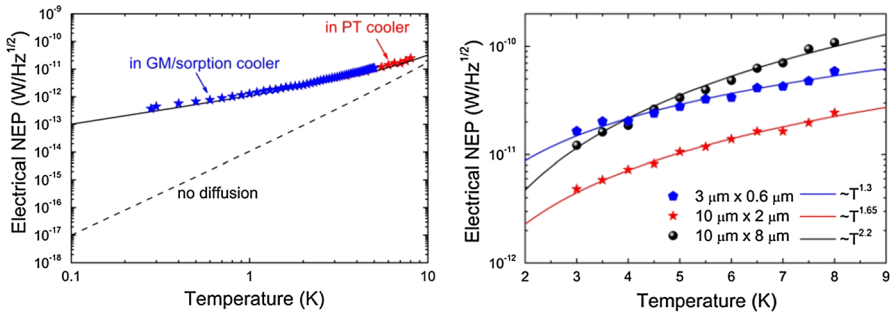
**Fig. 4** (Left) measured NEP (marked by star) of the graphene-based HEB. The solid line is the modeled data including the contribution from electron–phonon scattering, electron diffusion and microwave photon emission. The dash line is the modeled data not including electron diffusion. (Right) electrical NEP of the HEBs of different microbridge lengths (Color figure online)

where $G_{e-ph}$ and $G_{diff}$ are the electron–phonon and electron diffusion thermal conductance and $G_\gamma$ is the microwave photon emission conductance ($G_\gamma = k_B B$). At the temperature range studied in this work, the electron–phonon scattering is in the $T < T_{BG}$ (the Bloch–Gruneisen temperature) regime and $G_{e-ph} = 4\sum AT_e^3$, where $\sum$ and $A$ are the coupling constant and the area. The electron diffusion in a microbridge follows the Wiedemann–Franz relationship: $G_{diff} = 12L_0T_e/R$ [6], where $L_0$ and $R$ are the Lorenz constant and the electrical resistance of the microbridge. The prefactor 12 is the result of the temperature profile developed by uniform heating and by the presence of the thermal boundary condition of the contacts [10]. Figure 4 (left) shows the measured and modeled electrical NEP of the HEB at different bath temperatures, which are in good agreement. In the modeling, the coupling constant $\sum$ is estimated to be $100\,\text{mW/K}^4\text{m}^2$, close to that given in Ref. 6. Figure 4 (left) also shows the modeled NEP not including the contribution from electron diffusion. We can find that the NEP of the HEB is largely limited by electron diffusion and it can be improved by three orders at 0.3 K when the electron diffusion is eliminated. To further understand the thermal transport inside the graphene microbridge, three graphene-based HEBs of different microbridge lengths (varying from 0.6 to 8 μm) were measured. Figure 4 (right) shows the measured NEP of the HEBs at different bath temperatures. It can be seen that the temperature-dependent NEP can be fitted in terms of $T^n$, and the shorter the graphene microbridge is, the smaller the index $n$ is. It indicates that electron diffusion plays a more important role in shorter microbridges.

## 5 Conclusions

We have successfully developed a graphene -based terahertz HEB based on Johnson noise readout. The measured frequency response of the HEB shows a high coupling efficiency in the frequency range of 0.3–1.6 THz. At 3.0 K, the measured optical NEP of the HEB is about $5.6 \times 10^{-12}\,\text{W/Hz}^{0.5}$. From the measurements of the bolometers at different bath temperatures, we find that the NEP is largely limited by the heat diffusion

to the contact pads. Thus, the bolometer performance can be further improved if the electron diffusion is reduced (e.g., using superconducting contact pads).

## References

1. A.C. Betz, F. Vialla, D. Brunel, C. Voisin, M. Picher, A. Cavanna, A. Madouri, G. Feve, J.M. Berroir, B. Placais, E. Pallecchi, Phys. Rev. Lett. **109**, 056805 (2012)
2. C. Lee, J.Y. Kim, S. Bae, K.S. Kim, B.H. Hong et al., Appl. Phys. Lett. **98**, 071905 (2011)
3. A.E. Fatimy, R.L. Myers-Ward, A.K. Boyd, K.M. Daniels, D.K. Gaskill, P. Barbara, Nat. Nanotechnol. **11**, 335 (2016)
4. Q. Han, T. Gao, R. Zhang, Y. Chen, J.H. Chen, G.R. Liu, Y.F. Zhang, Z.F. Liu, X.S. Wu, D.P. Yu, Sci. Rep. **3**, 3533 (2013)
5. H. Vora, P. Kumaravadivel, B. Nielsen, X. Du, Appl. Phys. Lett. **100**, 153507 (2012)
6. K.C. Fong, K.C. Schwab, Phys. Rev. X **2**, 031006 (2012)
7. M.J. Wang, J.W. Wang, C.L. Wang, Y.Y. Chiang, H.H. Chang, Appl. Phys. Lett. **104**, 033502 (2014)
8. A.D. Semenov, H.W. Hubers, J. Schubert, G.N. Gol'tsman, A.L. Elaniev, B.M. Voronov, E.M. Gershenzon, J. Appl. Phys. **88**, 6758 (2000)
9. B.S. Karasik, C.B. McKitterick, D.E. Prober, J. Low Temp. Phys. **176**, 249 (2014)
10. D.E. Prober, Appl. Phys. Lett. **62**, 2119 (1993)